applied sciences

MDPI

Article

Numerical Modelling Study of Subsurface Drainage of Permeable Friction Course Considering Road Geometric Designs

Thi My Dung Huynh [1], Van Hiep Huynh [1], Minh Triet Pham [2], Kyra Kamille A. Toledo [3] and Tan Hung Nguyen [4,*]

[1] Department of Civil Engineering, School of Engineering and Technology, Tra Vinh University, Tra Vinh 87000, Vietnam; mydung@tvu.edu.vn (T.M.D.H.); hvhiep@tvu.edu.vn (V.H.H.)
[2] Akselos S.A., Ho Chi Minh City 700000, Vietnam; minhtriet240@gmail.com
[3] Faculty of Engineering, University of Santo Tomas, Manila 1008, Philippines; katoledo@ust.edu.ph
[4] Faculty of Civil Engineering, Can Tho University of Technology, Can Tho 900000, Vietnam
* Correspondence: nthung@ctuet.edu.vn; Tel.: +84-86-614-7457

Abstract: This study aimed to evaluate the subsurface drainage of a permeable friction course (PFC) via two-dimensional finite element analysis. To achieve the scope, PFCs with equivalent water flow paths of length values of 10, 15, 20, and 30 m and slope values of 0.5%, 2%, 4%, 6%, and 8% were modelled based on FEniCS and implemented entirely in Python programing language to extract the time for surface ponding according to a range of rainfall intensities. The results show that when the rainfall intensity and the length of equivalent water flow path of the PFC rose, the time for surface ponding decreased. For instance, with a rainfall intensity of 10 mm/h and a slope of 0.5%, when the length of equivalent water flow path increased by 20 m, the time for surface ponding dropped by 21 min. Moreover, when the slope of the equivalent water flow path and the thickness of the PFC increased, the time for surface ponding increased. For instance, with a rainfall intensity of 10 mm/h, and a PFC with an equivalent length of 10 m, when the slope increased by 16 times, the time for surface ponding increased more than two times. The current study highlights that the thickness of the PFC has the most influence on subsurface drainage. The findings of this study indicate that at high rainfall intensities, the subsurface drainage of a PFC is not sensitive to its geometric design. Further experimental investigations are needed to evaluate and validate the subsurface drainage of a PFC considering permeability, rutting, and environmental factors.

Keywords: subsurface drainage; time for surface ponding; permeable friction course; geometric design; Python; FEnics

check for updates

Citation: Huynh, T.M.D.; Huynh, V.H.; Pham, M.T.; Toledo, K.K.A.; Nguyen, T.H. Numerical Modelling Study of Subsurface Drainage of Permeable Friction Course Considering Road Geometric Designs. *Appl. Sci.* **2023**, *13*, 12428. https://doi.org/10.3390/app132212428

Academic Editors: Giuseppe Lacidogna and Luca Susmel

Received: 17 September 2023
Revised: 21 October 2023
Accepted: 7 November 2023
Published: 17 November 2023

1. Introduction

Several permeable friction courses (PFCs) have been widely used in permeable pavement systems to control rainwater quantity and quality during urbanization [1–3]. A PFC is a porous asphalt layer that is laid on the surface layer of a conventional impermeable asphalt pavement [4]. Porous asphalt is an asphalt material that is designed to have a high porosity so that water can infiltrate its pores and drain out vertically, laterally, or both. Hence, a PFC is used as a tool to drain out water and has the potential to reduce the peak flow of pollutants in rainwater [5–7].

Literature studies have reported that the properties of porous asphalt material (such as porosity and permeability) have a strong effect on the drainage of a PFC. In addition, the geometric design of the pavement, such as the longitudinal slope (S_y), cross slope (S_x), length (L), width (W), and thickness (T), also has remarkable drainage effects [8,9]. When using PFCs for stormwater management, the rainfall intensity (I) is an important factor that should be considered. To date, several studies have investigated the effects of these factors on the drainage of a PFC pavement. To achieve this, three methods have been used: the rainfall simulator experiment, laboratory experiment, and finite element analysis. The finite element analysis is a key method for observation because of its obvious benefits such as saving cost, saving time, and the high accuracy of the results [10].

Tan et al. [8] utilized a finite element program called Seep3D to observe the effect of pavement geometric design, including cross slope, longitudinal slope, thickness, width (S_x, S_y, T, and W), and rainfall intensity (I), on the drainage performance of a pavement. In their study, the permeability (k) of the porous asphalt was assumed to be 20 mm/s. The allowable rainfall intensity, which was the maximum rainfall intensity that could be applied over the pavement without surface ponding, was extracted according to the different values of the pavement geometric design. From the results of the study, a curve consisting of the ratio of the pavement thickness to the width (T/W) and the maximum allowable rainfall intensity was plotted. The outcome indicated that at a high value of cross slope (S_x), the longitudinal slope (S_y) did not seem to have any effect on the drainage of the pavement. In addition, the study found that a higher ratio of thickness to width (T/W) resulted in a lower effect on the longitudinal slope (S_y) of the drainage performance. In another study, Liu et al. [11] proposed a computational finite element model to predict the flow of water in a PFC during rainfall. The flow of water in the body of the PFC was estimated by a two-dimensional flow using the equation of diffusion, whereas the flow of water over the surface of the PFC was estimated by a three-dimensional flow using the equation of Richard. The study highlighted that the thickness (T) of the PFC pavement played an important role on the effect of the time for surface ponding. However, the thickness (T) of the PFC had a less significant effect on the phreatic line in its body.

In the permeable pavement design guide, the time at which surface ponding is initiated, known as the time for surface ponding (t_p), is a key factor in evaluating the peak flow of drainage in urban areas [12,13]. In low impact development techniques, t_p is called the delay time of peak flow, one of the typical factors for permeable pavement system design [14]. For transportation construction, it is also a critical factor for safety movements [15]. To date, there have not been many studies focused on the time for surface ponding of a PFC subjected to rainfall by finite element analysis. Rashid et al. [15] investigated the time for surface ponding of a PFC using a finite element analysis program called Flow 3D. The PFC was designed with a hexagonal modular pavement system for storage of water from rainfall. The results demonstrated that the time for surface ponding was obviously dependent on the rainfall intensity. Moreover, the hydrological performance of the hexagonal modular pavement system was affected by its permeability. The results illustrated that the hexagonal modular pavement system can be used as an effective tool in stormwater management by increasing the water storage capacity. Nguyen and Ahn [16] observed the time for surface ponding for a PFC using finite element analysis. In their study, the PFC had different lengths and slopes subjected to various rainfall intensities which were modelled and analyzed by the SVFlux 2D program. In the study, a series of analyses was examined using water flow length values of 10, 15, 20, and 30 m and slope values of 0.5%, 2%, 4%, 6%, and 8%. To determine the time for surface ponding, the PFCs were subjected to a series of rainfall intensities ranging from 10 to 120 mm/h. The results revealed that the time for surface ponding decreased when either the PFC length or rainfall intensity, or both, increased. Nevertheless, the time for surface ponding increased when the slope increased. The study provided a series of design charts to estimate the time for surface ponding for a PFC at given rainfall intensities. Recently, Hossam et al. [17] developed a three-dimensional finite element model to evaluate the impacts of PFC thickness, permeability, rainfall intensity, and traffic volume on seepage. From the analysis results, they implied that the considered factors, such as rainfall intensity, PFC thickness, and traffic volume, have a high impact on PFC seepage characteristics, except for PFC permeability. The implication was made because the PFC designed with porous asphalt, whose air void content was 16%, resulted in good drainage performance.

Previous studies have stated that the drainage performance of PFC is influenced by rainfall intensity, geometric design (e.g., cross slope, longitudinal slope, width, length), and its properties (e.g., air void, permeability). The time for surface ponding is a critical factor that has a significant effect on the hydrologic design for a PFC. Until recently, there has been little interest in the time for surface ponding of PFCs subjected to rainfall intensity. Thus, the purpose of the current study is to develop a finite element model to determine the time for surface ponding of a PFC subjected to rainfall intensity. Furthermore, this study examined the time for surface ponding of a PFC obtained from different water flow paths and subjected to different rainfall intensities. Based on the results, the subsurface drainage performance of the PFC was evaluated and discussed.

2. Subsurface Drainage and Time for Surface Ponding of a PFC

Generally, at a dry initial condition and constant rainfall intensity, the drainage of PFC for rainwater consists of two components: subsurface drainage and surface drainage. First, the rainwater infiltrates into the pores of the PFC and then drains out laterally through the side of the PFC, this drainage is known as subsurface drainage. The subsurface drainage of a PFC has a water shape in the PFC body that is laminar or between laminar and turbulent [9,18]. The head of the water flow (H) in a PFC body is captured in Figure 1. This value is a function of variations such as rainfall intensity, time of rainfall, permeability, and the geometric design of the PFC.

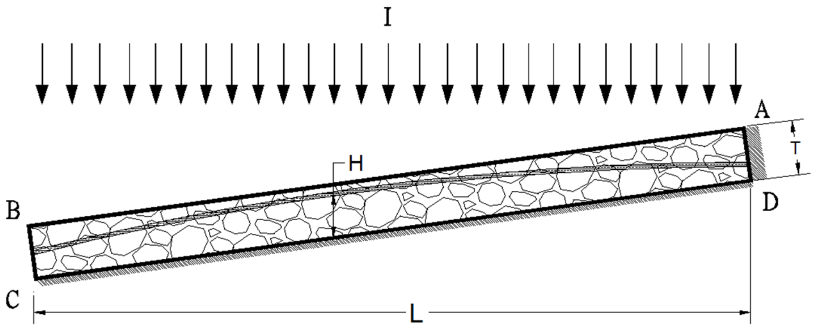

Figure 1. Head of water flow in a PFC body, after Ranieri, Nguyen and Ahn [9,16].

Second, during the rainfall process, as the pore of the PFC is filled with rainwater, the water head inside the PFC body gradually increases. When the water head reaches the surface of the PFC, surface runoff occurs, and then the rainwater starts to flow above the surface of the PFC; this drainage is known as the surface drainage. The duration from the time the rainfall starts to the surface ponding occurring over the surface of the PFC, is called the time for surface ponding (t_p).

3. Modeling of Subsurface Drainage of a Two-Dimensional PFC Based on Finite Element Analysis

3.1. Equivalent Water Flow Path for the Subsurface Drainage

A PFC is designed with a cross slope (S_x) and longitudinal slope (S_y) that can help drain rainwater effectively. According to Ranieri [9], the majority of water drains out through the equivalent water flow path, which is a result of the cross slope (S_x), longitudinal slope (S_y), and width (W) of the PFC. The equivalent water flow path of a PFC is described in Figure 2. This value can be determined by Equations (1) and (2):

$$S_R = \sqrt{S_x^2 + S_y^2} \tag{1}$$

$$L_R = W\sqrt{1 + \left({}^{S_y}/{}_{S_x}\right)^2} \tag{2}$$

Based on the manual of the American Association of State Highway and Transportation Officials, “Policy on Geometric Design of Highways and Streets” [19], and Equations (1) and (2), the equivalent water flow paths for the PFC including length (L_R) and slope (S_R), were forecasted. The results are shown in Figure 3.

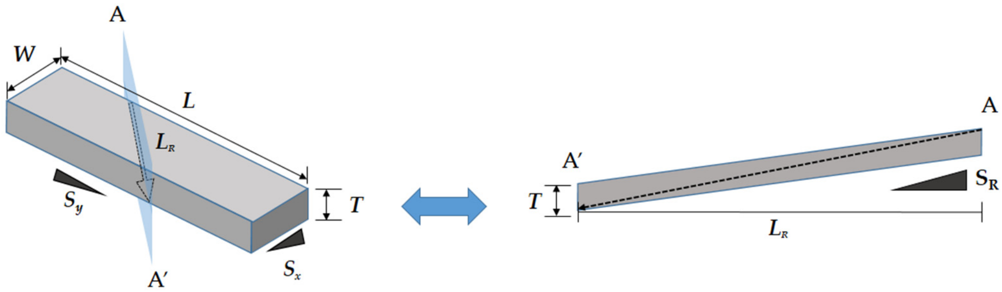

Figure 2. Equivalent water flow path: length (L_R) and slope (S_R), after Nguyen and Ahn [16].

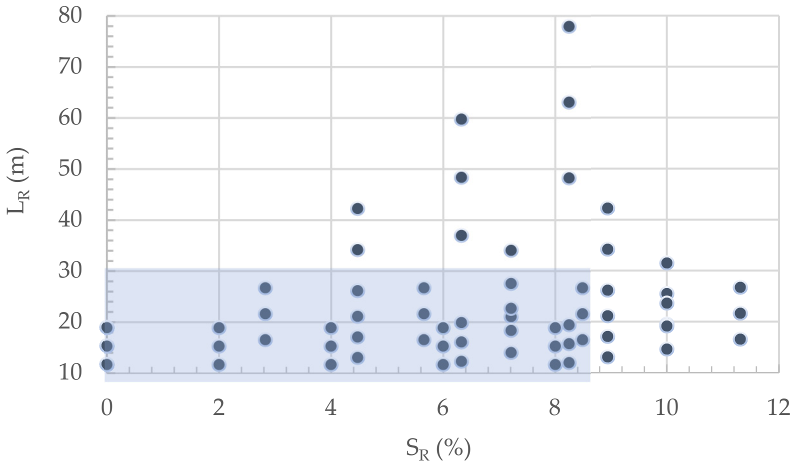

Figure 3. Equivalent water flow path includes length (L_R) and slope (S_R) values for the PFC.

3.2. Analysis Cases

In Figure 3, most of the results for the equivalent water flow path (L_R and S_R) are located in the shaded part. Hence, to assess the effect of geometric designs on the subsurface drainage of PFC, the current study chose the equivalent water flow path with a length (L_R) of 10 m, 15 m, 20 m, and 30 m and a slope (S_R) of 0.5%, 2%, 4%, 6%, and 8% for observation. For each analysis model, a rainfall intensity of 10 mm/h was initially calculated. Then, this value was increased in steps of 10 mm/h up to a value of 120 mm/h. For each scenario, the time for surface ponding (t_p) was recorded and reported. First, the effect of length (L_R) and slope S_R for the PFC with a thickness (T) of 50 mm on the subsurface drainage was observed. Details of the analysis cases are presented in Table 1.

Table 1. Analysis cases to observe the effect of equivalent water flow path, length (L_R) and slope (S_R).

Length, L_R (m)	Slope, S_R (%)	Rainfall Intensity, I (mm/h)
10, 15, 20, 30	0.5, 2, 4, 6, 8	10, 20, 30, 40, 50, 60, 70, 80, 90, 100, 110, 120

Previous studies showed that the subsurface drainage of a PFC significantly depends on the thickness (T) [8,9,20]. Secondly, this study also evaluated the impact of the thickness (T) of a PFC on its subsurface drainage. To achieve the scope, PFCs with different thickness T values were investigated. These values were chosen by following the literature studies [8,20]. Details of the analysis cases are shown in Table 2 below.

Table 2. Analysis cases to observe the effect of PFC thickness (T).

Length, L_R (m)	Thickness, T (mm)	Slope, S_R (%)	Rainfall Intensity, I (mm/h)
10	25, 50, 75	0.5, 2, 4, 6, 8	10, 20, 30, 40, 50, 60, 70, 80, 90, 100, 110, 120

3.3. Governing Equations and Variational Formulation

In this study, transient unsaturated seepage was utilized to model the subsurface drainage of the PFC. In the analysis, it was assumed that the water has a constant volume and is incompressible. The governing equation of the two-dimensional water flow is illustrated in Equation (3):

$$\frac{\partial}{\partial x}\left[k_x\frac{\partial h}{\partial x}+k_{vd}\frac{\partial u_w}{\partial x}\right]+\frac{\partial}{\partial y}\left[k_y\frac{\partial h}{\partial y}+k_{vd}\frac{\partial u_w}{\partial y}\right]=-\gamma_w m_2^w\frac{\partial h}{\partial t} \tag{3}$$

where k_x and k_y are the hydraulic conductivities in the horizontal and vertical directions, respectively, h is the total water head, k_{vd} is the vapor conductivity, u_w is the pore water pressure, γ_w is the unit weight of water, m_2^w is the coefficient of water storage obtained from the derivative of the soil–water characteristic curve (SWCC), and t denotes time.

It is of note that this study excludes the consideration of vapor flow and assumes isotropic permeability for the PFC pavement. Consequently, the partial differential equation in Equation (3) simplifies to the following:

$$\nabla\cdot(k\nabla h)+f=-\gamma_w m_2^w\frac{\partial h}{\partial t} \tag{4}$$

The SWCC presents the non-linear relationship between the volumetric water content and the suction in the PFC. In the current study, Van Genuchten's equation [21,22] was used to extract the SWCC, as shown in Equation (5):

$$\theta=\theta_r+\frac{\theta_s-\theta_r}{[1+(a\psi^n)]^m} \tag{5}$$

where θ represents volumetric water content, θ_s is the saturated volumetric water content, θ_r is the residual volumetric water content, Ψ signifies the soil suction, and a, n, and m are material (fitting) parameters.

The drainage process within the PFC is treated as a time-dependent problem governed by the partial differential equation (PDE) presented in Equation (4). To solve this, the time derivative using an implicit Euler approximation was discretized, leading to Equation (6):

$$\nabla\cdot\left(k\nabla h^{n+1}\right)+f^{n+1}=-\gamma_w m_2^w\left(\frac{h^{n+1}-h^n}{\Delta t}\right) \tag{6}$$

where n denotes the time level and Δt is the time discretization parameter. This equation can be effectively solved using the finite element method (FEM). The weak formulation of Equation (6) is expressed in Equation (7):

$$\int\limits_{\Omega} hvd\Omega+\Delta tk\int\limits_{\Omega}(\nabla h\cdot\nabla v)d\Omega=\int\limits_{\Omega} vh^{n+1}d\Omega+\Delta t\int\limits_{\Gamma} f^{n+1}vd\Gamma \tag{7}$$

where, for all v belonging to a suitable function space, Ω represents the domain, and $d\Omega$ is the differential volume element. In this study, an FEM solver was developed using FEniCS [23] and implemented entirely in Python programing language.

3.4. Boundary Conditions

To simulate subsurface drainage in the body of a PFC, the model incorporated three primary types of boundary conditions, denoted as "natural," "review," and "zero-flux" conditions. The schematic representation of these conditions is depicted in Figure 1. Initially, the "natural" boundary condition was assigned to the bottom of the PFC, specifically along the CD line, where it was assumed that the rainfall infiltrated through the surface and gradually accumulated at the bottom of the PFC. Subsequently, the "review" boundary condition was designated for the BC line, corresponding to the location of subsurface drainage. In seepage analysis, the "review" boundary condition is defined as follows: (i) if the pressure head (h) is negative, the boundary condition results in zero flux; (ii) if h is positive, it corresponds to a negative flux that effectively reduces the pore-water pressures at the surface to zero. Finally, the zero-flux boundary conditions were imposed on the surface AB line and the upper AD line, where drainage was deemed infeasible.

3.5. PFC Parameters

In this study, the permeability of a PFC was assumed to be isotropic and chosen based on the result in the study of Yoo et al. [24], which was 10 mm/s. Literature studies demonstrated that when there was no rainfall in a dry condition, the PFC had a suction pressure. Therefore, in the PFC body, there was a negative value of pore water pressure [25]. Thus, the initial pore water pressure in the PFC body in the current study was set to a negative value within the range of the residual zone. Based on the SWCC, the value of the negative pore water pressure was chosen. The SWCC parameters for PFC in this study followed those results in the study of Lim and Kim [26]. In their study, they experimented on pervious concrete samples by using Fredlund's device. Then, the SWCC parameters were extracted through the equation of Fredlund and Xing [27]. The SWCC parameters are presented in Table 3. From these parameters, the graph of the SWCC curve is shown in Figure 4.

Table 3. SWCC parameters for the PFC pavement, after Lim and Kim [26].

Volumetric Water Content, θ_s (%)	Residual Volumetric Water Content, θ_r (%)	Material Parameters		Soil suction, Ψ (kPa)
		a	n	
20	0.001	2.23	1.63	0.01

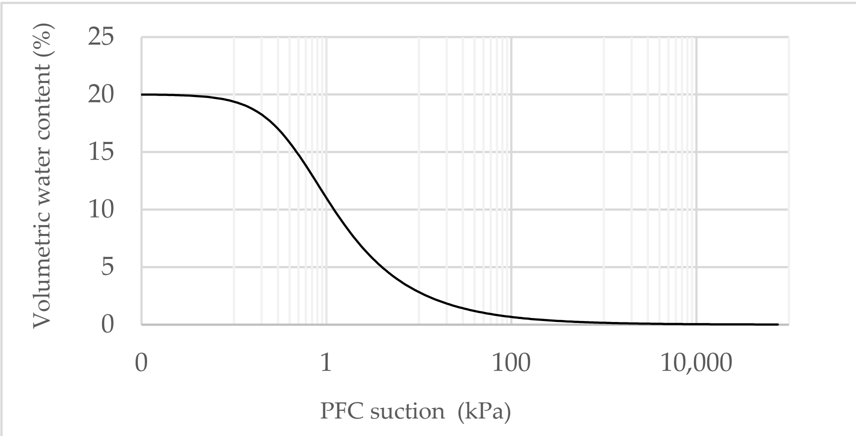

Figure 4. SWCC curve for the PFC, after Lim and Kim [26], Nguyen and Ahn [16].

Based on the SWCC curve for PFC in Figure 4, the suction pressure value was selected as 200 kPa to ensure that the PFC was initially dry before rainfall occurred.

4. Results and Discussion

4.1. Time for Surface Ponding

A series of rainfall intensities from 10 mm/h to 120 mm/h, with a step of 10 mm/h, was applied to the PFC model to extract the time for surface ponding (t_p). The results are displayed in Table 4.

Table 4. Time for surface ponding (t_p) for the PFC at various rainfall intensity values (I).

L_R (m)	S_R (%)	Time for Surface Ponding, t_p (min)											
		I = 10 (mm/h)	20	30	40	50	60	70	80	90	100	110	120
10	0.5	81	39	25	19	15	12	10	9	8	7	6	5
	2	86	40	26	19	15	12	11	9	8	7	6	5
	4	96	45	29	21	17	14	11.2	10	9	8	7	6
	6	114	52	34	24	19	15.5	13	12	10	9	8	7
	8	189	80	50	36	28	23	19	16	14	13	11	10
15	0.5	72	35	23	17	13	11	9	8	7	6	5.5	5
	2	76	37	24	18	14	11	9.5	8	7	6	5.5	5
	4	84	40	26	19	15	12	10	9	8	7.5	6.3	5.5
	6	99	46	30	22	17	14	12	10	9	8	7	6.2
	8	153	67	43	31	24	20	17	14	13	11	10	9
20	0.5	67	32	21	16	12	10	9	7	6.5	5.7	5	4
	2	70	34	22	16	12.5	10.5	9	7.5	7	6	5	4
	4	77	37	24	18	14	11.5	10	8	7	6.3	5.5	5
	6	90	42	28	20	16	13	11	9	8	7	6	5.7
	8	136	61	39	28	22	18	15	13	11.5	10	9	8
30	0.5	60	29	19	14	11	9	8	7	6	5	4.5	4
	2	64	31	20	15	12	10	8	7	6	5	4.5	4
	4	67	33	22	16	12.5	10.3	8.5	7.3	6.4	5.5	5	4.7
	6	80	38	25	18	14.1	12	9.5	8.3	7.2	6.1	6	5
	8	116	53	34	25	19.1	16	13.2	12	10	9	8	7

It is apparent from Table 4 that a PFC with different geometric designs obtains various values of time for surface ponding. When the rainfall intensity increases, there is a downward trend in the time for surface ponding. The present finding in this study is in agreement with Mahmoud et al. [28] and Nguyen et al. [29] which showed that as the rainfall intensity increased, the time for surface ponding decreased. It could be concluded that the subsurface drainage of the PFC is strongly dependent on the rainfall intensity and the geometric design of the PFC.

The present study was successful as it was able to determine the time for surface ponding in several cases where the other study could not. In the study of Nguyen and Ahn [16], the time for surface ponding of the PFC at low rainfall intensity could not be determined since the SVFlux 2D program took such a long time to analyze. This study has gone some way towards filling the gap where the time for surface ponding could not be extracted.

4.2. Effect of Length of Equivalent Water Flow Path on the Subsurface Drainage of a PFC

To observe the effect of PFC geometric designs on subsurface drainage, the curves depicted in Figure 5 present the relationship between the length of the equivalent water flow path (L_R) and the time for surface ponding (t_p) according to the different rainfall intensity values (I). The curves show that there is an inverse relationship between L_R and t_p; remarkably, the higher value of L_R resulted in a lower value of t_p. For example, for I = 10 mm/h and S_R = 0.5%, as L_R increased by 20 m (from 10 m to 30 m), t_p dropped by 21 min (from 81 min to 60 min). The behavior indicated that surface ponding could occur faster for the PFC that had a longer L_R. This implication is consistent with that found in the studies of Nguyen and Ahn [16] and Liu et al. [30]. According to Luo et al. [31], a possible explanation for this might be that the PFC with a longer L_R could accumulate more water from rainfall than the one with a shorter L_R. Hence, PFCs with shorter L_R performed better than the PFCs with longer L_R in subsurface drainage.

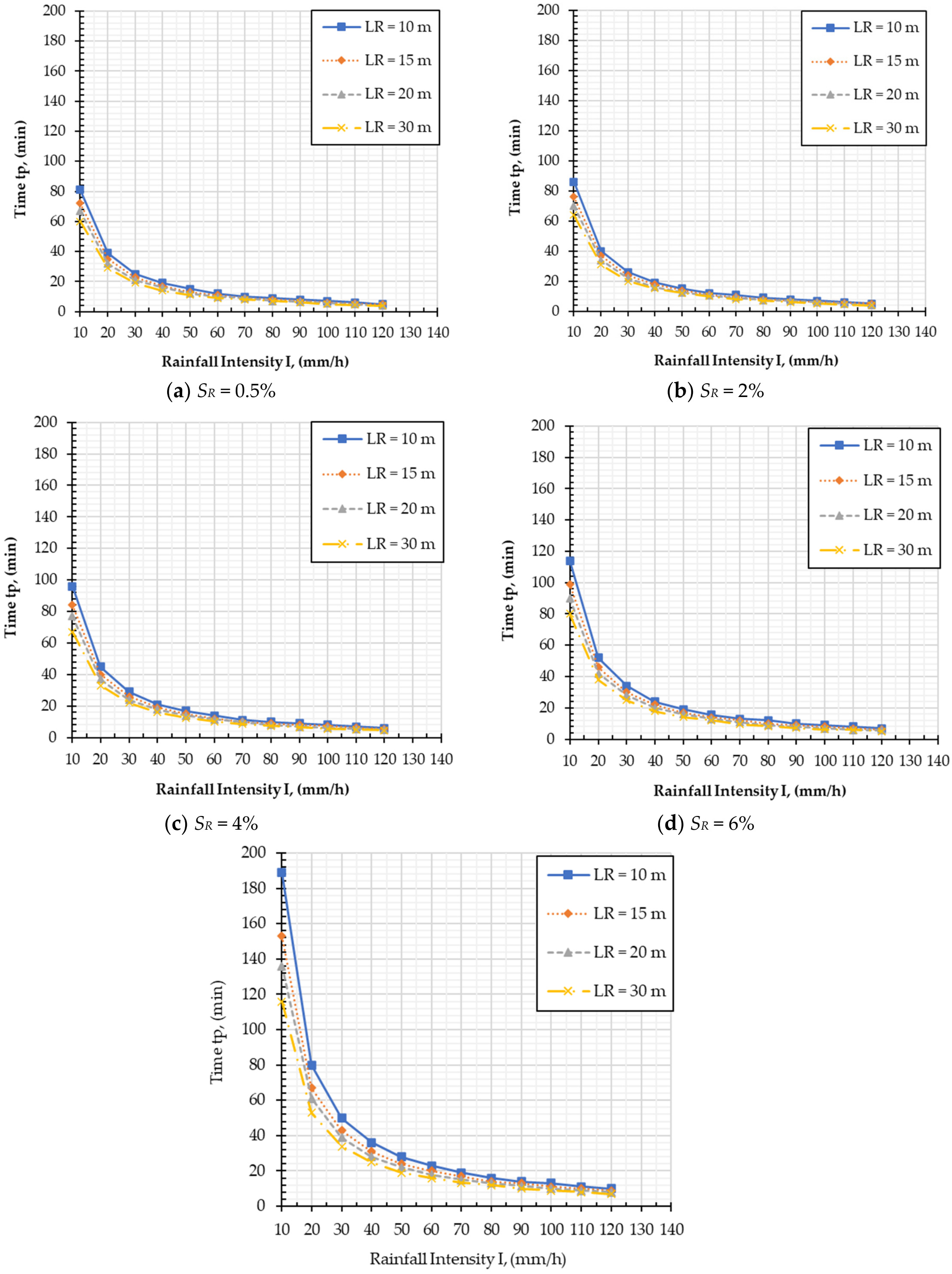

(**a**) S_R = 0.5% (**b**) S_R = 2% (**c**) S_R = 4% (**d**) S_R = 6% (**e**) S_R = 8%

Figure 5. Relationship between the time for surface ponding (t_p) and rainfall intensity (I) with different length (L_R) values.

The PFC with a shorter L_R provided a wide range of time for surface ponding (t_p). The evidence of this can be clearly seen in the case at S_R = 4%; with the PFC with L_R = 10 m, at I = 10 mm/h, and I = 50 mm/h, t_p decreased by 79 min (from 96 to 17 min). Moreover, the values of t_p for L_R = 15, L_R = 20, and L_R = 30 m were 69, 63, and 54.5 min, respectively. Thus, the conclusion was that the PFC with a shorter L_R seems to be more sensitive to rainfall intensity values than the one with a longer L_R. It is of note that the change in L_R values did not have a significant effect on the results of t_p. This behavior could be seen clearly at high rainfall intensities. In Figure 5, the PFC with different L_R values at the high rainfall intensities from 80 to 120 mm/h resulted in close t_p values. Thus, it could be concluded that L_R had a low impact on the subsurface drainage of the PFC.

4.3. Effect of Slope of Equivalent Water Flow Path on the Subsurface Drainage of a PFC

The effects of the slope of the equivalent water flow path (S_R) on PFC subsurface drainage were also investigated. The curves in Figure 6 illustrate the relationship between the slope of the equivalent water flow path (S_R) and the time for surface ponding (t_p), according to the different rainfall intensity values (I). The observation showed that the increase in S_R resulted in an increase of t_p. For instance, for the PFC with L_R = 10 m and I = 10 mm/h, when S_R increased by 16 times (from 0.5% to 8%), t_p increased more than two times (from 81 to 189 min). This performance is consistent with that of Tan et al. [8], Nguyen and Ahn [16]. The results indicated that the PFC with a higher S_R exhibits a higher subsurface drainage capacity than the one with a lower S_R. This rather contradictory result may be due to the speed of drainage. Alireza et al. [32] speculated that a higher slope could help increase the speed of drainage water in the PFC body and cause a lower water head in the PFC body.

The varieties of slope S_R showed a lower impact on the subsurface drainage for the PFC with a longer L_R. By way of illustration, at I = 10 mm/h, when the value of S_R increases two times (from 2% to 4%), for L_R = 10 m, t_p increased significantly by 10 min (from 86 to 96 min), but for L_R = 15, L_R = 20, and L_R = 30 m, this value increased by only 8 min, 7 min, and 3 min, respectively. Thus, it can be concluded that the subsurface drainage of the PFC with a longer L_R is less sensitive to the slope S_R. It is of note that the change in S_R values had a significant effect on the results of t_p. PFCs with different S_R provided a wide range of results for t_p. Thus, it could be concluded that S_R had a high impact on the subsurface drainage of PFCs. Surprisingly, the results of t_p of PFCs with different geometric designs are almost close at high rainfall intensities. This indicates that the subsurface drainage of PFCs at high rainfall intensity has a similar response, regardless of the geometric designs.

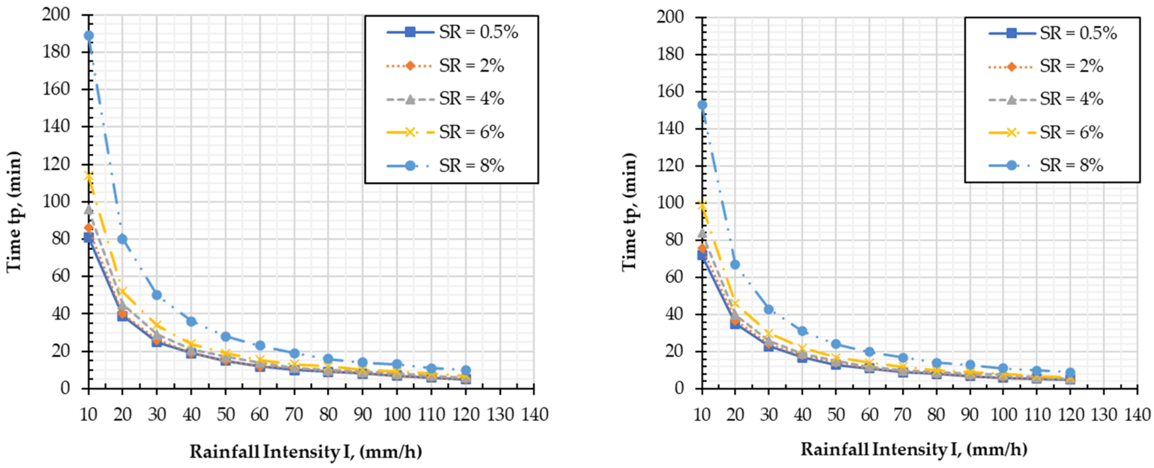

(**a**) L_R = 10 m (**b**) L_R = 15 m

Figure 6. *Cont.*

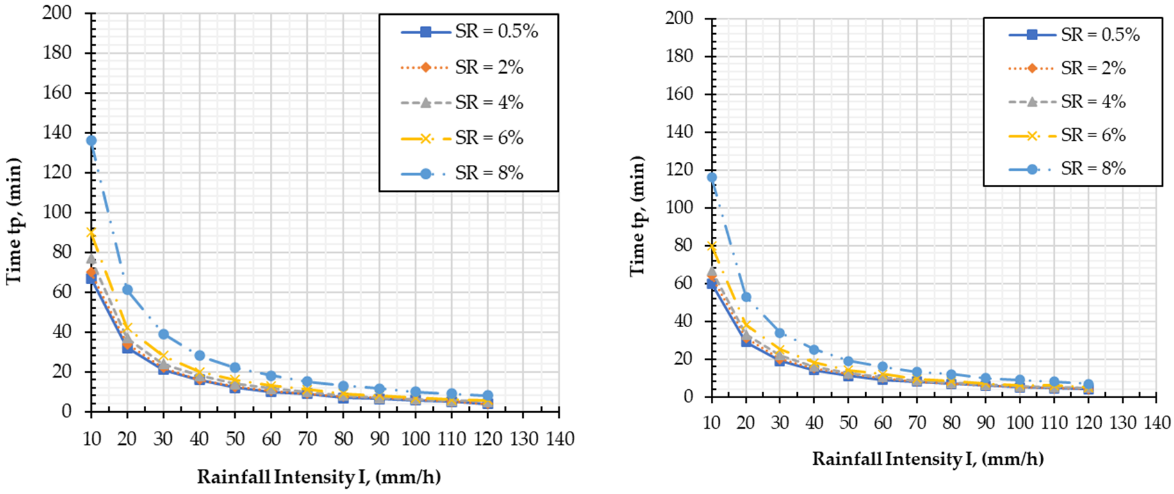

(**c**) L_R = 20 m (**d**) L_R = 30 m

Figure 6. Relationship between the time for surface ponding for PFC (t_p) and rainfall intensity (I) with different slope (S_R) values.

4.4. Effect of Thickness on the Subsurface Drainage of a PFC

The effect of thickness (T) of the PFC on its subsurface drainage was evaluated. Figure 7 describes the relationship between the time for surface ponding (t_p) and rainfall intensity values (I) in the consideration of thickness (T) for PFCs having an equivalent length (L_R) of 10 m.

In Figure 7, it can be seen that the thickness (T) has a strong effect on the results of the time for surface ponding t_p of a PFC. As the thickness T of the PFC increased, the results of the time for surface ponding t_p increased sharply. It is apparent that as T increases by a factor of two, t_p only doubles. Moreover, as T increases by a factor of three, t_p rises more than six times. The evidence of this can be clearly seen in the case of the PFC at I = 30 mm/h, when T increased two times from 25 to 50 mm, t_p also increased two times (from 13 to 26 min). At the same condition, when T increased three times from 25 to 75 mm, t_p rose about 7.3 times (from 13 to 95 min). This behavior implied that the thickness T of the PFC has a strong effect on its subsurface drainage. The finding further supports the idea of Chen et al. [33], who found that the thickness of the PFC had the most remarkable effect on the permeability of the PFC.

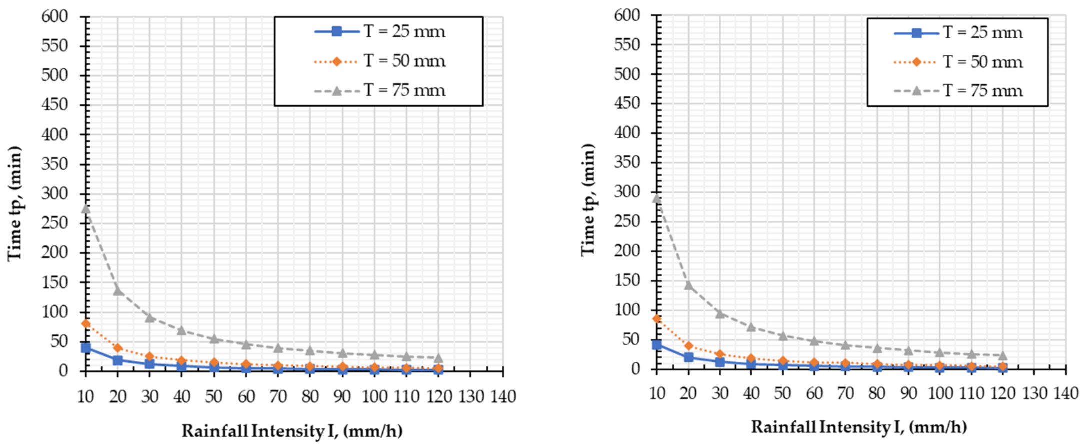

(**a**) S_R = 0.5% (**b**) S_R = 2%

Figure 7. *Cont.*

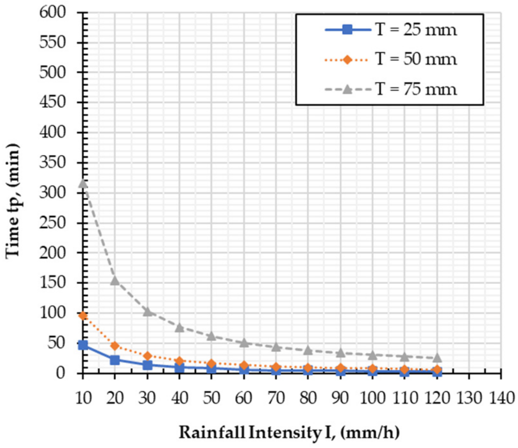

(**c**) S_R = 4%

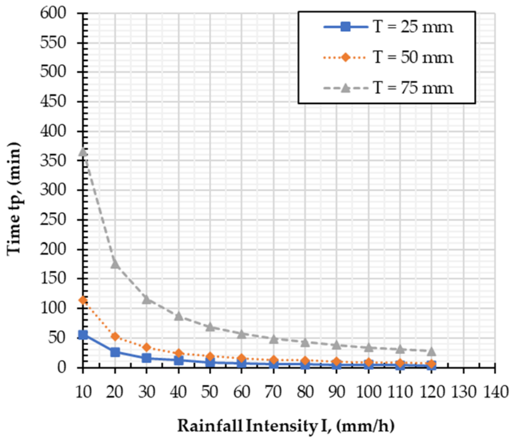

(**d**) S_R = 6%

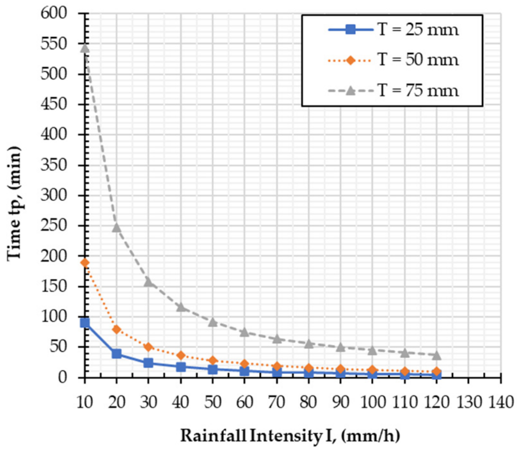

(**e**) S_R = 8%

Figure 7. Relationship between the time for surface ponding (t_p) of the PFC and rainfall intensity (I) with different thickness (T) values.

This study found that the subsurface drainage of the PFC is more sensitive to its thickness T at lower rainfall intensity values. For instance, at I = 20 mm/h and S_R = 4%, the results for the time for surface ponding t_p for PFC with T = 25 mm and 50 mm are 22 and 45 min, respectively. They vary significantly by 23 min. However, at I = 120 mm/h, the results are 2.7 and 6 min. The difference in the values of t_p is only 3.3 min, which are close to each other. The conclusion was drawn that the thickness T of the PFC does not seem to significantly affect the subsurface drainage of the PFC at high rainfall intensity. A similar conclusion was found in the study of Nguyen and Ahn [16].

5. Conclusions

In this study, the subsurface drainage of a PFC with various equivalent water flow paths, including length and slope, was observed via two-dimensional finite element analysis. A series of analyses was conducted for PFCs with equivalent water flow path length values of 10, 15, 20, and 30 m and slope values of 0.5%, 2%, 4%, 6%, and 8%. The PFCs were subjected to a range of rainfall intensities, from 10 to 120 mm/h, with a step of 10 mm/h to extract the time for surface ponding. Based on the results and discussions, the following conclusions were drawn.

PFCs subjected to various rainfall intensity values resulted in various times for surface ponding. In general, when the rainfall intensity increased, there was a downward trend in the time for surface ponding of the PFC. The geometric designs of PFCs had a remarkable impact on the subsurface drainage of the PFC. PFCs with different geometric designs provide a wide range of time for surface ponding values. Among the three factors of the geometric design of the PFC, thickness has the most influence on subsurface drainage. It is of note that at a high rainfall intensity, the geometric design of the PFC does not seem to affect significantly the subsurface drainage of the PFC.

The observation of the subsurface drainage of the PFC according to the equivalent water flow path including the length L_R and the slope S_R showed that, with L_R, it has an inversely proportional trend, while with S_R, it has a similar trend. Another highlighted implication of this study is that the PFC with a shorter L_R appears to be more sensitive to rainfall intensity and slope values. The present study provided additional evidence with respect to the effect of PFC thickness. As the thickness T increased, the results of the time for surface ponding t_p increased gradually. The current study only examined the subsurface drainage of PFCs using two-dimensional finite element analysis based on FEniCS and implemented it entirely in the Python programing language. Further experimental investigations are needed to evaluate the subsurface drainage of PFCs, considering other factors such as permeability, rutting, and environmental factors.

Author Contributions: Conceptualization, T.H.N. and M.T.P.; methodology, T.H.N.; software, M.T.P.; validation, M.T.P. and T.H.N.; formal analysis, M.T.P.; investigation, T.H.N.; resources, M.T.P.; data curation, T.M.D.H.; writing—original draft preparation, T.H.N.; writing—review and editing, K.K.A.T. and T.H.N.; visualization, M.T.P.; supervision, T.H.N.; project administration, T.M.D.H.; funding acquisition, V.H.H. All authors have read and agreed to the published version of the manuscript.

Funding: This research was fully supported by Tra Vinh University under grant contract number 247/2022/HĐ.HĐKH&ĐT-ĐHTV.

Institutional Review Board Statement: Not applicable.

Informed Consent Statement: Not applicable.

Data Availability Statement: Data are contained within the article.

Acknowledgments: The authors would like to thank the Tra Vinh University.

Conflicts of Interest: Author Minh Triet Pham was employed by the company Akselos S.A. The remaining authors declare that the research was conducted in the absence of any commercial or financial relationships that could be construed as a potential conflict of interest.

References

1. Chu, L.; Tang, B.; Fwa, T. Evaluation of functional characteristics of laboratory mix design of porous pavement materials. *Constr. Build. Mater.* **2018**, *191*, 281–289. [CrossRef]
2. Wu, H.; Yu, J.; Song, W.; Zou, J.; Song, Q.; Zhou, L. A critical state-of-the-art review of durability and functionality of open-graded friction course mixtures. *Constr. Build. Mater.* **2020**, *237*, 117759. [CrossRef]
3. Zhang, L.; Ye, Z.; Shibata, S. Assessment of rain garden effects for the management of urban storm runoff in Japan. *Sustainability* **2020**, *12*, 9982. [CrossRef]
4. Manrique-Sanchez, L.; Caro, S. Numerical assessment of the structural contribution of porous friction courses (PFC). *Constr. Build. Mater.* **2019**, *225*, 754–764. [CrossRef]
5. Eck, B.J.; Winston, R.J.; Hunt, W.F.; Barrett, M.E. Water quality of drainage from permeable friction course. *J. Environ. Eng.* **2012**, *138*, 174–181. [CrossRef]
6. Berbee, R.; Rijs, G.; De Brouwer, R.; van Velzen, L. Characterization and treatment of runoff from highways in the Netherlands paved with impervious and pervious asphalt. *Water Environ. Res.* **1999**, *71*, 183–190. [CrossRef]
7. Roseen, R.M.; Ballestero, T.P.; Houle, J.J.; Avellaneda, P.; Briggs, J.; Fowler, G.; Wildey, R. Seasonal performance variations for storm-water management systems in cold climate conditions. *J. Environ. Eng.* **2009**, *135*, 128–137. [CrossRef]
8. Tan, S.; Fwa, T.; Chai, K. Drainage considerations for porous asphalt surface course design. *Transp. Res. Rec.* **2004**, *1868*, 142–149. [CrossRef]
9. Ranieri, V. Runoff control in porous pavements. *Transp. Res. Rec.* **2002**, *1789*, 46–55. [CrossRef]
10. Ali, M.H. Finite Element Analysis is A Powerful Approach to Predictive Manufacturing Parameters. *J. Univ. Babylon Eng. Sci.* **2018**, *26*, 229–238.
11. Liu, X.; Chen, Y.; Shen, C. Coupled two-dimensional surface flow and three-dimensional subsurface flow modeling for drainage of permeable road pavement. *J. Hydrol. Eng.* **2016**, *21*, 04016051. [CrossRef]
12. NRCS; USDA. *Urban Hydrology for Small Watersheds-Technical Release 55*; US Department of Agriculture Natural Resources Conservation: Washington, DC, USA, 1986.

13. Eisenberg, B.; Lindow, K.C.; Smith, D.R. *Permeable Pavements*; American Society of Civil Engineers: Reston, VA, USA, 2015.
14. LeFevre, N.-J.B.; Watkins, D.W., Jr.; Gierke, J.S.; Brophy-Price, J. Hydrologic performance monitoring of an underdrained low-impact development storm-water management system. *J. Irrig. Drain. Eng.* **2010**, *136*, 333–339. [CrossRef]
15. Rashid, M.; Abustan, I.; Hamzah, M. Numerical simulation of a 3-D flow within a storage area hexagonal modular pavement systems. *IOP Conf. Ser. Earth Environ. Sci.* **2013**, *16*, 012056. [CrossRef]
16. Nguyen, T.H.; Ahn, J. Numerical study on the hydrologic characteristic of permeable friction course pavement. *Water* **2021**, *13*, 843. [CrossRef]
17. Abohamer, H.; Elseifi, M.A.; Mayeux, C.; Cooper, S.B., III; Cooper, S., Jr. Investigating the Seepage Characteristics of an Open-Graded Friction Course Using Finite Element Modeling. *Transp. Res. Rec.* **2023**, 03611981231168103. [CrossRef]
18. Kovács, G. *Seepage Hydraulics*; Elsevier: Amsterdam, The Netherlands, 2011.
19. AASHTO. *Policy on Geometric Design of Highways and Streets*; American Association of State Highway Transportation Officials: Washington, DC, USA, 2001; p. 158.
20. Ranieri, V.; Ying, G.; Sansalone, J. Drainage modeling of roadway systems with porous friction courses. *J. Transp. Eng.* **2012**, *138*, 395–405. [CrossRef]
21. Van Genuchten, M.T. A closed-form equation for predicting the hydraulic conductivity of unsaturated soils. *Soil Sci. Soc. Am. J.* **1980**, *44*, 892–898. [CrossRef]
22. Fredlund, M. *User's Manual for SVFlux, Saturated-Unsaturated Numerical Modeling*; SoilVision Systems: Saskatoon, SK, Canada, 2010.
23. Alnæs, M.; Blechta, J.; Hake, J.; Johansson, A.; Kehlet, B.; Logg, A.; Richardson, C.; Ring, J.; Rognes, M.E.; Wells, G.N. The FEniCS project version 1.5. *Arch. Numer. Softw.* **2015**, *3*, 20553. [CrossRef]
24. Yoo, J.; Nguyen, T.H.; Lee, E.; Lee, Y.; Ahn, J. Measurement of Permeability in Horizontal Direction of Open-Graded Friction Course with Rutting. *Sustainability* **2020**, *12*, 6428. [CrossRef]
25. Si, C.; Chen, E.; You, Z.; Zhang, R.; Qiao, P.; Feng, Y. Dynamic response of temperature-seepage-stress coupling in asphalt pavement. *Constr. Build. Mater.* **2019**, *211*, 824–836. [CrossRef]
26. Lim, B.K.; Kim, Y.T.; Department of Ocean Engineering, Pukyong National University, Busan, South Korea. Personal Communication, 2012.
27. Fredlund, D.G.; Xing, A. Equations for the soil-water characteristic curve. *Can. Geotech. J.* **1994**, *31*, 521–532. [CrossRef]
28. Mahmoud, A.A.; Mbengue, M.T.M.; Hussain, S.; Abdullahi, M.A.; Beddal, D.; Abba, S.I. Investigation for Flood Flow quantification of Porous Asphalt with Different Surface and Subsurface Thickness. *Knowl. Based Eng. Sci.* **2023**, *4*, 78–89.
29. Nguyen, H.T.; Nguyen, T.P.; Phan, T.N.; Tran, P.T.; Nguyen, P.B. Investigation on hydrologic performance of pervious concrete pavement by finite element analysis. *Tra Vinh Univ. J. Sci.* **2022**, *12*, 56–63. [CrossRef]
30. Liu, L.; Wu, S.; Yao, G.; Zhang, J.; Montalvo, L.; Tahri, O. Developing In-Situ Permeability and Air Voids Requirements for Open-Graded Friction Course Pavement: Case Study. *Int. J. Civ. Eng.* **2022**, *20*, 107–114. [CrossRef]
31. Luo, W.; Wang, K.C.; Li, L.; Li, Q.J.; Moravec, M. Surface drainage evaluation for rigid pavements using an inertial measurement unit and 1-mm three-dimensional texture data. *Transp. Res. Rec.* **2014**, *2457*, 121–128. [CrossRef]
32. Pourhassan, A.; Gheni, A.A.; ElGawady, M.A. Water film depth prediction model for highly textured pavement surface drainage. *Transp. Res. Rec.* **2022**, *2676*, 100–117. [CrossRef]
33. Chen, X.; Wang, H.; Li, C.; Zhang, W.; Xu, G. Computational investigation on surface water distribution and permeability of porous asphalt pavement. *Int. J. Pavement Eng.* **2022**, *23*, 1226–1238. [CrossRef]